Accepted Manuscript



Interaction analyses of 14-3-3ζ, Dok1 and phosphorylated integrin β cytoplasmic tails reveal a bi-molecular switch in integrin regulation

Deepak Chatterjee, Areetha D'Souza, Yaming Zhang, Wu Bin, Suet-Mien Tan, Surajit Bhattacharjya

PII: S0022-2836(18)30601-6
DOI: doi:10.1016/j.jmb.2018.09.008
Reference: YJMBI 65876

To appear in: *Journal of Molecular Biology*

Received date: 8 June 2018
Revised date: 14 September 2018
Accepted date: 14 September 2018

Please cite this article as: Deepak Chatterjee, Areetha D'Souza, Yaming Zhang, Wu Bin, Suet-Mien Tan, Surajit Bhattacharjya , Interaction analyses of 14-3-3ζ, Dok1 and phosphorylated integrin β cytoplasmic tails reveal a bi-molecular switch in integrin regulation. Yjmbi (2018), doi:10.1016/j.jmb.2018.09.008

This is a PDF file of an unedited manuscript that has been accepted for publication. As a service to our customers we are providing this early version of the manuscript. The manuscript will undergo copyediting, typesetting, and review of the resulting proof before it is published in its final form. Please note that during the production process errors may be discovered which could affect the content, and all legal disclaimers that apply to the journal pertain.

ACCEPTED MANUSCRIPT

Interaction analyses of 14-3-3ζ, Dok1 and phosphorylated integrin β cytoplasmic tails reveal a bi-molecular switch in integrin regulation

Deepak Chatterjee[1], Areetha D'Souza[1], Yaming Zhang[1,2], Wu Bin[1,2], Suet-Mien Tan[1,*] smtan@ntu.edu.sg, Surajit Bhattacharjya[1,2,*] surajit@ntu.edu.sg

[1]School of Biological Sciences, Nanyang Technological University, 60 Nanyang Drive, Singapore 637551, Singapore

[2]NTU Institute of Structural Biology, Nanyang Technological University, 59 Nanyang Drive, Singapore 636921, Singapore

[*]Corresponding authors at: 60 Nanyang Drive, Singapore, 637551.

Abstract

Integrins are hetero-dimeric (α and β subunits) type I transmembrane proteins that facilitate, cell adhesion and migration. The cytoplasmic tails (CTs) of integrins interact with a plethora of intra-cellular proteins that are required for integrin bidirectional signaling. In particular, the β CTs of integrins are known to recruit a variety of cytosolic proteins that often have overlapping recognition sites. However, the chronological sequence of β CTs/cytosolic proteins interactions remains to be fully characterized. Previous studies have shown that the scaffold protein 14-3-3ζ binds to phosphorylated β CTs in activated integrins whereas interactions of Dok-1 with phosphorylated β CTs maintained integrins in the resting state. In this study, we examined the binding interactions between 14-3-3ζ, Dok1 and phosphorylated integrin β2 and β3 CTs. We show that the scaffold protein 14-3-3ζ interacts with the phosphotyrosine binding (PTB) domain of Dok1 even in the absence of the phosphorylated

ACCEPTED MANUSCRIPT

integrin β CTs. The interactions were mapped onto the β-sheet region of the PTB domain of Dok1. Further, we provide evidence that the 14-3-3ζ/Dok1 binary complex is able to bind to their cognate phosphorylated sequence motifs in the integrin β CTs. We demonstrate that, Thr phosphorylated pTTT β2 CT or pTST β3 CT can bind to 14-3-3ζ that is in complex with the Dok1 PTB domain. Whereas, Ser phosphorylated β2 CT or Tyr phosphorylated β3 CT interacted with Dok1 in 14-3-3ζ/Dok1 complex. Based on these data, we propose that 14-3-3ζ/Dok1 complex could serve as a molecular switch providing novel molecular insights towards the regulating integrin activation.

Graphical abstract

Keywords: integrins; NMR; protein-protein interaction; 14-3-3; Dok1

Introduction

Integrins are transmembrane proteins composed of α and β subunits [1]. Each subunit contains a large extracellular region, a single-pass transmembrane segment, and a cytoplasmic tail (CT). Integrins are linker proteins that connect the cytoskeleton with the extracellular matrix. In metazoans, integrins are crucial receptors mediating cell adhesion, migration and cell-cell communication [2,3]. The binding of integrins to their ligands require conformational change regulated through allostery [4,5]. Integrins are bi-directional signaling receptors [6,7]. Integrin inside-out signaling describes the process by which cytosolic protein regulators bind to the integrin CTs and induce long-range conformational change that promotes integrin ligand-binding [8]. Integrin outside-in signaling commonly describes post-ligand binding event in which integrin clustering triggers intracellular signaling [9].

ACCEPTED MANUSCRIPT

A rapidly growing list of cytosolic proteins directly interact with integrin CTs [8], which suggest intricate regulatory mechanisms. The integrin β CTs contain two highly conserved NxxY/F (x: other amino acid) motifs [7]. The NxxY/F motif that is proximal to the plasma membrane is the binding site of the cytoskeletal protein talin-1 (henceforth referred to as talin). Binding of talin head domain to the integrin cytoplasmic tail disrupts a salt-bridge connecting the integrin α and β CTs, leading to their separation followed by integrin activation [10]. Dok-1 belongs to the family of Dok adaptor proteins that negatively regulates immune cell signaling and Ras-ERK signaling, and they serve as tumor suppressors [11-13]. Dok1 contains an N-terminal pleckstrin homology (PH) domain followed by a phosphor-tyrosine binding (PTB) domain and SH2 and SH3 sites. Dok1 is a negative regulator of integrin activation by competing with talin for the same integrin binding site [14]. Dok1 binding to the integrin β3 membrane proximal NPLY747 motif has been shown to be dependent on the phosphorylation of Y747 [14]. A phosphorylation switch model was proposed in which Dok1 binding to integrin membrane proximal NxxpY prevents talin binding to the same site, and the dephosphorylation of Nxx(p)Y is required for the release of Dok1 prior to talin-induced integrin activation. In our previous study, we proposed an alternative model to clarify the mechanism by which Dok1 binds to integrin β2 CT containing a membrane proximal NPLF754 that is not amenable to phosphorylation [15]. In this alternative model, Ser745 and Ser756 that flank the integrin β2 NPLF754 motif serve as the phosphorylation switch.

Another notable feature in the CTs of integrin β2, β3, β6 and β7 is the presence of a TT/ST motif that lies between the two NxxY/F motifs [7]. The scaffold protein 14-3-3ζ, a member of the pS/T-binding family of proteins, positively regulates the ligand-binding properties of β2 integrins by binding to its pT758TT motif [16-18]. It was proposed that 14-3-3ζ promotes β2

ACCEPTED MANUSCRIPT

integrin clustering based on the crystal structure of 14-3-3ζ homodimer in association with two integrin β2 cytoplasmic tail peptides containing pT758TT [18]. Given that the T758TT motif in integrin β2 is close to the NPLF754 motif, which is also the binding site of talin and Dok-1, the spatio-temporal organization of these molecules in the vicinity of the integrin cytoplasmic tail warrants investigation. We previously showed that 14-3-3ζ, talin and integrin β2 CT can form a ternary complex, and 14-3-3ζ binding to the integrin β2 CT results in the repositioning of talin head domain in the complex [19]. We also provided evidence that the binding of 14-3-3ζ to integrin β2 CT containing pT758TT prevents Dok1 interaction with the β2 tail [19]. In this study, we report a novel interaction between 14-3-3ζ and Dok1. Our data suggested that the complex can potentially function as a switch that regulates integrin function.

Results

The PTB domain of Dok1 and 14-3-3ζ form a complex: Interactions between the PTB domain of Dok1 and 14-3-3ζ were investigated by ^{15}N-^{1}H HSQC NMR, ^{15}N transverse relaxation measurement and isothermal titration calorimetry (ITC). A series of ^{15}N-^{1}H HSQC spectra of ^{15}N labelled PTB domain of Dok1 were acquired at different molar ratios, 1:0, 1:0.2, 1:0.5, 1:0.8, 1:1 and 1:2, of Dok1 and 14-3-3ζ. Fig. 1a shows overlay of ^{15}N-^{1}H HSQC spectra of the PTB domain of Dok1 in free solution (in blue) and in the presence of 14-3-3ζ at 1:1 (red) and 1:2 (green) ratios. The ^{15}N-^{1}H HSQC cross-peaks of the PTB domain of Dok1 delineated diminution of intensity upon inclusion of 14-3-3ζ, demonstrating interactions between the two proteins. The intensity reduction of ^{15}N-^{1}H cross-peak of each amino acid was estimated at 1:0.5 molar ratio of Dok1 and 14-3-3ζ (Fig. 1b). ^{15}N-^{1}H HSQC cross-peaks of residues showing $\leq$0.2 residual intensity are marked onto the three-dimensional structure of the PTB domain of Dok1 (Fig. 1c). The PTB domain fold of the

ACCEPTED MANUSCRIPT

Dok1 contains seven stranded β-sheet topology and a long C-terminal helix [20]. Most of the residues located on the β-sheet structures of the PTB domain were found to be relatively more perturbed compared to the C-terminal long helix (Fig. 1c). Notably, the residues belonging to the β strand 5 were also less perturbed (Fig. 1c). Interestingly, peptide ligand binding pocket of the PTB domain of Dok1 is maintained by the C-terminal helix and the adjacent β strand 5. ^{15}N transverse relaxation rate ($R_2 = 1/T_2$) is a sensitive parameter for inter-molecular interactions, conformational and chemical exchange processes [21]. We compared R_2 of free PTB domain and in the presence of sub-stoichiometric concentration, 1:0.1 molar ratio, of 14-3-3ζ enabling estimation of R_2 for most of the residues (Fig. 2). As expected, several residues, throughout the sequence, of the PTB domain showed an increase in R_2 as a result of interactions with 14-3-3ζ (Fig. 2). Lower R_2 values were also estimated for fewer residues e.g. His18, Arg24, G68 of the PTB domain, indicating differential changes in conformational dynamics (Fig. 2). The affinity and thermodynamic parameters of binding of 14-3-3ζ and PTB domain were determined from ITC (Fig. 3, Table 1). 14-3-3ζ and Dok1 PTB domain interaction was found be exothermic based on ITC therograms (Fig. 3, top panel). The apparent dissociation constant, K_d, of the interactions was estimated to be 294 μM (Table 1). The binding between 14-3-3ζ and the PTB domain was driven by a favorable change in enthalpy, indicating potential involvement of polar interactions in stabilizing the complex. Collectively, the aforementioned data demonstrate a novel interaction between the scaffold protein 14-3-3ζ and the adaptor protein Dok1 PTB domain in the absence of phosphorylation.

14-3-3ζ/Dok1 complex can bind phosphorylated integrin β3 CT: We then examined whether 14-3-3ζ/Dok1 PTB domain complex can associate with phosphorylated integrin β2 and β3 CTs (Table 2). Phosphorylation of the Tyr747 residue at the membrane proximal

ACCEPTED MANUSCRIPT

NPLY^{747} motif of integrin β3 CT enables Dok1 binding [14, 22, 23]. It has also been shown that 14-3-3ζ interacts with β3 CT upon phosphorylation of the conserved Thr777 residue at the T^{777}ST motif [24,25]. Fig 4a shows overlay of ^{15}N-^{1}H HSQC spectra of the PTB domain of Dok1 in free solution (blue), in the presence of pYβ3 CT (red) and pYβ3 CT+14-3-3ζ (green). In agreement with previous reports [14,22], Dok1 PTB interacted with pYβ3 CT as evident from the disappearance or broadening of several ^{15}N-^{1}H HSQC cross-peaks (Fig. 4a, Supplementary Fig. S1). Further, the addition of 14-3-3ζ caused more changes to the ^{15}N-^{1}H HSQC spectra of Dok1 PTB as many more HSQC cross peaks disappeared (Fig. 4a). We further examined ^{31}P NMR of pYβ3 CT in the presence of 14-3-3ζ and Dok1+14-3-3ζ complex (Fig. 4b). The ^{31}P NMR signal of pYβ3 CT moved significantly downfield when in complex with PTB domain of Dok1 suggesting accommodation of the pY residue into the binding pocket of Dok1. However, no chemical shift change of ^{31}P resonance of pYβ3 CT was detected in the presence of 14-3-3ζ, suggesting a lack of interaction (Fig. 4b). In the presence of an equimolar mixture of Dok1+14-3-3ζ, the ^{31}P resonance of pYβ3 CT shifted upfield as compared to that of Dok1/pYβ3 CT complex (Fig. 4b). We then examined the binding affinity of pYβ3 CT with Dok1 and 14-3-3ζ by ITC. pYβ3 CT interacted with Dok1 PTB (Fig. 4c) and the Dok1+14-3-3ζ complex (Fig. 4d). The binding parameters are provided in Table 1. pYβ3 binds to the binary complex of Dok1+14-3-3ζ with higher affinity (K_d ~ 16.5 μM) as compared to Dok1 PTB (K_d ~ 41.8 μM). Previous NMR study reported a K_d of 37.1 μM for pYβ3 CT and Dok1 PTB interaction [14].

We further investigated the interactions between pTβ3 CT with Dok1 PTB and Dok1+14-3-3ζ complex by ^{15}N-^{1}H HSQC of PTB domain and ^{31}P NMR (Fig. 5). Fig. 5a shows the overlay of ^{15}N-^{1}H HSQC spectra of PTB domain of Dok1, in free solution, and in the presence of pTβ3 CT only and with pTβ3+14-3-3ζ. Clearly, HSQC spectra of the Dok1 PTB

ACCEPTED MANUSCRIPT

domain remained largely unchanged in the presence of pTβ3, only few residues L52, L53, R58 and Y65 showed ≤0.025 ppm change of weighted chemical shift (Supplementary Fig. S2). Whereas further inclusion of 14-3-3ζ caused disappearance of most of the HSQC peaks due to signal broadening (Fig. 5a). ^{31}P NMR spectra of pTβ3 CT were acquired in the presence of Dok1 PTB domain and Dok1 PTB+14-3-3ζ at different molar ratios (Fig. 5b). ^{31}P resonance of pTβ3 CT shifted upfield in the presence of Dok1 PTB+14-3-3ζ as compared to Dok1 alone (Fig. 5b). ^{15}N-^{1}H HSQC titration data suggest that Dok1 PTB domain interacts with 14-3-3ζ in the presence of either pTβ3 CT or pYβ3CT. On the other hand, ^{31}P NMR data suggest that pTβ3 CT is able to bind to 14-3-3ζ in the presence of Dok1 PTB. In addition, pYβ3 CT interacted with Dok1 PTB in the presence of 14-3-3ζ. Taken together, these data provide evidence that pYβ3 CT or pTβ3 CT interacts binary complex of 14-3-3ζ/Dok1 PTB.

14-3-3ζ/Dok1 complex can bind phosphorylated integrin β2 CT: We also investigated interactions of pTβ2 CT (phosphorylated at residue Thr 758) and pSβ2 CT (phosphorylated at residue Ser 756) with 14-3-3ζ/Dok1 PTB complex. Binary complexes of 14-3-3ζ/pTβ2 CT and Dok1 PTB/pSβ2 CT have been characterized [15,18]. Fig. 6a shows the overlay of ^{15}N-^{1}H HSQC spectra of PTB domain of Dok1 in isolation, and in the presence of pTβ2 CT and pTβ2CT+14-3-3ζ. After addition of pTβ2 CT, limited spectral changes were observed for Dok1 PTB indicating potential low affinity interactions (Supplementary Fig. S3). However, HSQC spectral changes of the PTB domain, in terms of resonance broadening, were apparent upon inclusion of 14-3-3ζ. ^{31}P NMR spectral changes showed binding of 14-3-3ζ and 14-3-3ζ+Dok1 complex with the phosphorylated pTβ2 CT (Fig. 6b). It should be noted that 14-3-3ζ binds to pTβ2 CT at higher affinity, estimated K_d 4.9 μM [19], compared to 14-3-3ζ/Dok1 PTB interactions (Table 1). The interaction affinity of 14-3-

ACCEPTED MANUSCRIPT

3ζ/Dok1 complex with pTβ2 is K_d ~ 12.6 μM as determined by ITC, which is comparable with the affinity of 14-3-3ζ with pTβ2 CT (Fig. 6c, Table 1). These results suggest that 14-3-3ζ can simultaneously bind to pTβ2 and Dok1 PTB in a ternary fashion.

We next examined the binding of pSβ2 CT with Dok1 and Dok1/14-3-3ζ. ^{15}N-^{1}H HSQC spectra of the PTB domain of Dok1 showed discernable chemical shift changes of residues involved in binding upon addition of pSβ2 CT (Fig. 7a). NMR studies of Dok1 PTB/pSβ2 CT interaction has been reported [15]. As expected, in the presence of 14-3-3ζ, ^{15}N-^{1}H HSQC cross-peaks of the Dok1 were broadened and many cross-peaks remained invisible, typifying interactions of Dok1 and 14-3-3ζ in the presence of pSβ2 CT (Fig. 7a). Further, ^{31}P NMR spectra of pSβ2 CT in complexes of Dok1 PTB and 14-3-3ζ/Dok1 PTB were acquired (Fig. 7b). The chemical shift of the ^{31}P resonance of pSβ2 CT showed a downfield shift, compared to the free pSβ2 CT peptide, in complex with Dok1 PTB (Fig. 7b). The ^{31}P chemical shift was only slightly perturbed in the presence of the Dok1+14-3-3ζ complex (Fig. 7b). These data suggest that Dok1 PTB can bind to pSβ2 CT while retaining interactions with 14-3-3ζ. Binding interactions of pSβ2 CT with Dok1 PTB and preformed complex of 14-3-3ζ/Dok1 PTB were assessed by ITC (Fig. 7c). ITC thermograms showed binding induced exothermic heat release. The pSβ2 CT interacted with Dok1 PTB/14-3-3ζ complex with an estimated K_d ~ 298 μM (Table 1). However, binding parameters of Dok1 PTB/pTβ2 CT cannot be reliably estimated due to lack of saturation, which resulted poor fitting of the ITC data (Fig. 7c).

Molecular models of 14-3-3ζ/Dok1 PTB and phosphorylated β CTs: A molecular model of 14-3-3ζ and Dok1 PTB was generated by using HADDOCK based docking with chemical shift perturbation data (see materials and methods). In the complex, the dimeric 14-3-3ζ can accommodate two subunits of Dok1 PTB domain in a symmetrical manner (Fig. 8a).

ACCEPTED MANUSCRIPT

Note, a binding stoichiometry of 2.5 (Dok1 PTB:14-3-3ζ) was estimated from ITC (Table 2). The PTB domain of Dok1 binds to the concave face of the helical bundle of 14-3-3ζ. The docked structure disclosed that 14-3-3ζ binds to Dok1 PTB utilizing its secondary binding region or the C-terminal I helix that would essentially allow the phosphorylated peptides to interact at the primary binding site without any steric conflicts (Fig. 8). The interactions between the 14-3-3ζ and Dok1 PTB appeared to be sustained by multiple mutual interactions. A long helix at the C-terminal, spanning residues E208-L227, of 14-3-3ζ establishes packing and polar interactions with Dok1 PTB domain (Fig. 8b and 8c). Residues Tyr211 and Lys212 of 14-3-3ζ are found to be in close proximity of Trp 156 of PTB, indicating potential aromatic/aromatic packing and cation/π interactions. The side-chain/side-chain non-polar packing between residues Leu216 of 14-3-3ζ and Leu188 of PTB domain may further complement the aromatic cluster (Fig. 8b). Cation/π type interactions may be forming between residues Arg222 of 14-3-3ζ and Tyr174 of Dok1. Potential polar interactions can also formed between residues of 14-3-3ζ and Dok1 PTB Thr215/Ser173, Asp223/Thr187 and Thr226/Gln171 (Fig. 8b and 8c). In order to ascertain implications of residues Trp156, Tyr174 and Leu188 (Val188 in human sequence), of Dok1 interacting with 14-3-3ζ, an Ala mutant construct (W156A, Y174A, Val188A) of Dok1 PTB was further examined by ITC and NMR experiments. ^{15}N-^{1}H HSQC spectra revealed folded structure of the mutant Dok1 PTB domain (Supplementary Fig. S4). ^{15}N-^{1}H HSQC spectral changes of the mutant Dok1 PTB were observed after inclusion of 14-3-3ζ, at 1:0.5 and 1:1 ratios (Supplementary Fig. S4). However, ^{15}N-^{1}H HSQC resonance perturbations of the mutant Dok1 PTB appeared to be limited compared to the native Dok1 PTB, as many more ^{15}N-^{1}H correlations could be detectable (Supplementary Fig. S4). ITC data showed weaker interactions between the mutant Dok1 PTB, with 14-3-3ζ (Supplementary Fig. S5). Binding parameters could not be

ACCEPTED MANUSCRIPT

reliably due to lack of saturation (Supplementary Fig. S5). The molecular model of 14-3-3ζ and Dok1 PTB was used to dock phosphorylated pTβ2 and a Tyr phosphorylated peptide from RET. The docking was guided by the crystallographic structure of 14-3-3ζ/pTβ2 [18] and PTB Dok1/pY peptide [20]. Both the phosphorylated peptides were successfully docked, without any steric conflicts, onto the 14-3-3ζ/Dok1 complex (Fig. 8d).

Discussion

Integrin activation, clustering and the assembly of integrin-adhesome are regulated by a large number of cytosolic proteins that interact directly with the β CTs of integrins [5,6]. Cytosolic proteins 14-3-3ζ and Dok1 are negative and positive regulators, respectively, of integrin activation [13,14,17,18]. Phosphorylation of integrin β3 and β2 CTs has been shown to regulate their interactions with Dok1 and 14-3-3ζ [17,18,24,25]. The integrin binding sites of 14-3-3ζ and Dok1 are in close proximity, prompting us to ask whether they can form a ternary complex with the integrin β CT. In this study, we demonstrated a novel interaction between 14-3-3ζ and the Dok1 PTB domain. A large body of biophysical and structural data described interactions of 14-3-3 family of proteins with widely different phosphorylated (pT or pS) proteins and peptides [26-28]. However, 14-3-3ζ has also been shown to bind non-phosphorylated proteins [29-33]. Based on our data, the interaction between 14-3-3ζ and the Dok1 PTB domain is independent of phosphorylation. Although the interaction between them is relatively weak (K_d of 294 μM), it is comparable to binding affinities reported for 14-3-3ζ with other phosphorylated and non-phosphorylated ligands [26]. In order to obtain atomistic resolution of their interacting interface, we performed crystallization screens of 14-3-3ζ and Dok1 PTB domain complex but were unsuccessful (data not shown). Note, to-date, 3-D

ACCEPTED MANUSCRIPT

structure of a complex of 14-3-3ζ and phosphorylated serotonin N-acetyltransferase protein domain has been determined [34]. This structure showed that primary and secondary interactions of 14-3-3ζ with a large protein domain.

The cytoskeletal protein filamin binds to unphosphorylated β CTs in the resting state of integrins, whereas, phosphorylation of Thr residue at the T(T/S)T motif not only inhibited filamin interactions but also recruits the scaffold protein 14-3-3ζ in activated β2 integrins [18,35]. Ternary complex formation between filamin A IgFLN21 and the CTs of integrin αIIbβ3 was shown to maintain integrin αIIbβ3 in an inactive state [36], whereas ternary complex formation involving integrin β3 CT, talin and kindlin-3 plays a role in integrin activation [37]. In this study, we provide evidence supporting a ternary complex that consists of 14-3-3ζ, Dok1 PTB domain and integrin β CT. A noteworthy feature of this complex is that it comprises both negative and positive regulators of integrin activation. Based on our data, both 14-3-3ζ and Dok1 PTB need not simultaneously bind the integrin β CT. Instead, when Dok1 PTB binds to integrin β CT, 14-3-3ζ is tethered to Dok1 PTB without interacting with the integrin β CT. Conversely, when 14-3-3ζ binds integrin β CT, Dok1 PTB is tethered to 14-3-3ζ without interacting with the integrin β CT. The interaction between Dok1 PTB or 14-3-3ζ with integrin β CT is dependent on site specific phosphorylation of the integrin β CT.

Our data establish a new paradigm for integrin regulation that involves multi-protein complex. We propose a regulatory complex that contains a positive regulator 14-3-3ζ and negative regulator Dok1. An illustration of the possible mechanism by which this complex regulates integrin activation, using β2 integrin as an example, is shown (Fig. 9). In this model, 14-3-3ζ and Dok1 form a complex, which is bound to the integrin β2 CT pS756 via Dok1 PTB domain. Together with filamin A (IgFLNa21), a negative regulator of integrin activation, Dok1 suppresses integrin activation by preventing talin binding. In response to cellular

ACCEPTED MANUSCRIPT

stimuli that promote integrin activation, kindlin-3 binds to the integrin β2 CT along with migfilin, displacing filamin A (IgFLNa21) from its integrin binding site. Concomitantly, dephosphorylation of pS756 and phosphorylation of T758 in integrin β2 CT by yet to be identified phosphatase and kinase promote a switchover from Dok1 to 14-3-3ζ binding. The release of filamin from the integrin β2 CT also allows talin binding. We have shown previously that both talin and 14-3-3ζ can bind to the integrin β2 CT simultaneously [19]. Hypothetically, the pre-assembled Dok1 and 14-3-3ζ complex would favor a fast switchover because of the proximity of the molecules to the integrin β2 CT, facilitating rapid integrin activation after chemokine stimulation in immune cells.

In conclusion, underpinning molecular nature of the multi-protein complexes interacting with CTs of integrins may glean novel mechanistic insights. This work demonstrated a binary complex between the scaffold protein 14-3-3ζ and adaptor protein Dok1 that interacted with the cognate phosphorylated β CTs of β2 and β3 integrins. We surmise that acting as a molecular switch 14-3-3ζ/Dok1 complex could efficiently control activation and repression of the bidirectional signaling of integrins.

Materials and Methods

Protein expression and purification: Synthetic genes of human Dok1 PTB domain (Q154-G256), mutant Dok1 PTB (W156A, Y174A and V188A) and 14-3-3ζ (M1-S230) were subcloned into the pET14b vector with an N-terminal His-tag. *Escherichia coli* Rosetta cells were transformed with the expression plasmid and grown at 37 °C either in LB or M9 medium containing [^{15}N] ammonium chloride (Cambridge Isotope Laboratories). Expression of recombinant proteins were induced by adding 0.5 mM IPTG to cells (OD_{600} 0.6–0.7) followed by incubation for 10–12 h at 16 °C. Cells were centrifuged and re-suspended in

ACCEPTED MANUSCRIPT

buffer A (100 mM sodium phosphate and 300 mM NaCl, pH 8.0) followed by affinity purification on a Nickel-NTA column (Qiagen). His-tagged proteins were eluted in buffer A containing 500 mM imidazole and dialyzed against buffer B 20 mM sodium phosphate and 50 mM NaCl (pH 6.5), 2 mM DTT. Protein samples were further purified by gel filtration either in buffer B or buffer C 20 mM Tris-HCL and 50 mM NaCl (pH 6.5), 2 mM DTT on a Hiload Superdex 75 16/26 GL preparative column that was connected to an AKTA FPLC UPC-900 system (GE Healthcare UK Ltd., England). Proteins were eluted at a flow rate of 0.3 ml/min and monitored by absorbance at $\lambda = 276$ nm.

Synthetic peptides: All synthetic peptide were purchased from GLBioChem, Shanghai, China and were further purified using reverse phage HPLC (Waters^{TM} 2489). Lyophilized and molecular weight of the peptides was confirmed by mass spectrometry.

NMR spectroscopy: All NMR experiments were performed either on a Bruker Avance II 700 or 600 MHz spectrometer equipped with an actively shielded cryoprobe. NMR data were processed using NMRPIPE or Topspin 3.0 and analyzed by Sparky (T.D. Goddard and D.G. Kneller, University of California, San Francisco). The chemical shifts were directly or indirectly referenced to 2,2-dimethyl-2-silapentane-5-sulfonate. ^{15}N–^{1}H HSQC spectra for ^{15}N-labeled Dok1 was acquired at a concentration of 0.1 mM in buffer B, 20 mM sodium phosphate, 50 mM NaCl at pH 6.5. For interaction studies by NMR titration, ^{15}N–^{1}H HSQC spectra of Dok1 samples were recorded after 10 min of equilibration with sequential addition of binding partners. Stock solutions of 2.1 mM, 2.8 mM, 2.3 mM and 3.1 mM of pYβ3 CT, pTβ3 CT, pSβ2 CT, and pTβ2 CT, respectively, were used to titrate against 0.1 mM ^{15}N-labeled Dok1 at different molar ratios (1:0.5, 1:1, 1:1.5, 1:2 and 1:3). ^{15}N-^{1}H HSQC titrations were carried out with above mentioned stock of ligand in solutions containing equimolar mixture (0.1 mM) of ^{15}N-labeled Dok1 and unlabeled 14-3-3ζ. For, protein-protein interactions, 0.1 mM ^{15}N-Dok1 was titrated with unlabelled 14-3-3ζ at molar ratio of 1:0.1,

ACCEPTED MANUSCRIPT

1:0.2, 1:0.5, 1:1, 1:2 and 1:3. ^{15}N-^{1}H HSQC spectra of mutant Dok1 PTB, 0.2 mM, were acquired in free solutions and in the presence of 14-3-3ζ at 0.5 and 1.0 molar ratios. The transverse relaxation (T_2=1/R_2) rates of ^{15}N nuclei of backbone of Dok1, in presence of 14-3-3ζ at low ratio of 1:0.1, were determined by collecting a series of ^{15}N–^{1}H HSQC spectra of 0.1mM Dok1, with sensitivity enhancement in 600 MHz spectrometer at 298 K temperature. R_2 measurements were acquired with delays of 14.4, 28.8, 43.2, 57.6, 72.0, 86.4, 100.8, 115.2, 129.6, 144.0, and 158.4 ms. R_2 values were estimated by fitting the cross-peak intensities to a mono-exponential function as in I = A*exp(R*t), where I, A, R, and t represent signal intensity, constant, relaxation value, and time point, respectively. ^{31}P NMR spectra of pYβ3 CT, pSβ2 CT, pTβ3 CT and pTβ2 CT were recorded on a Bruker DRX 400 spectrometer with dual channel RT probe at 298 K and at concentrations of 0.25 mM of peptides. Data acquisition and processing were performed with the Topspin software (BRUKER) suite. ^{31}P NMR titration of all peptides acquired in a buffer containing 20 mM Tris and 50 mM NaCl (pH 6.0) using stock solutions of Dok1 and 14-3-3ζ, 0.68 mM and 0.77 mM, respectively.

Isothermal titration calorimetry (ITC): All samples were prepared in 20 mM sodium phosphate and 50 mM NaCl (pH 6.5). ITCs were performed in a VP-ITC200 instrument at 298 K. For 14-3-3ζ and Dok1/phosphorylated CTs binding, fixed amounts of CT peptides were injected into cell (200 µl) containing either Dok1 or 14-3-3ζ or equimolar 14-3-3ζ:Dok1. For protein-protein interaction, fixed concentrations of Dok1 PTB or mutant Dok1 PTB (W156A, Y174A and V188A) were injected into cell (200 µl) containing 14-3-3ζ. Typically, the first injection of 0.2 µl was followed by 19 injections of 2 µl, with 120s time delay between two injections, and samples stirred at a speed of 750 rpm. For heat of dilution proteins or peptides were into buffer. All raw data were processed using MicroCal Origin software

Docking of Dok1 with 14-3-3ζ: The model of Dok1 (PDB: 1uef) [20] and 14-3-3ζ (PDB:

ACCEPTED MANUSCRIPT

2v7d) [18] complex was derived using HADDOCK program (http://haddock.science.uu.nl/) based on chemical shift changes and line broadening of Dok1 in presence of 14-3-3ζ at 1:0.5. Docking was carried out using the x-ray structure of mouse Dok1 PTB complex with RET peptide [38]. The model structure was validated using ADIT Validation Server from the Protein Data Bank (PDB).

Acknowledgement: This work was supported by grants (ARC18/13, RG140/17) from the Ministry of Education (MOE), Singapore.

References

1. Hynes RO. Integrins: bidirectional, allosteric signaling machines. Cell 2002;110:673-687.
2. Johnson MS, Lu N, Denessiouk K, Heino J, Gullberg D. Integrins during evolution: evolutionary trees and model organisms. Biochimica et biophysica acta 2009;1788: 779-789.
3. Sebe-Pedro A, Ruiz-Trillo I. Integrin-mediated adhesion complex. Commun Integr Biol. 2010;3:475-477.
4. Luo BH, Carman CV, Springer TA. Structural basis of integrin regulation and signaling. Annu. Rev. Immunol. 2007;25:619-647.
5. Arnaout MA, Goodman SL, Xiong JP. Structure and mechanics of integrin-based cell adhesion. Curr. Opin. Cell Biol. 2007;19:495-507.
6. Qin J, Vinogradova O, Plow EF. Integrin bidirectional signaling: a molecular view. PLoS Biol. 2004;2:e169.
7. Tan SM. The leucocyte β2 (CD18) integrins: the structure, functional regulation and signalling properties. Bioscience Reports 2012;32:241-269.
8. Harburger DS, Calderwood DA. Integrin signalling at a glance. J. Cell Sci. 2009;122:159-163.
9. Carman CV, Springer TA. Integrin avidity regulation: are changes in affinity and conformation underemphasized? Curr. Opin. Cell Biol. 2003;15:547-556.
10. Shattil SJ, Kim C, Ginsberg MH. The final steps of integrin activation: the end game. Nat Rev Mol Cell Biol 2010;11:288-300.
11. Mashima, R., Arimura, S., Kajikawa, S., Oda, H., Nakae, S., and Yamanashi, Y. Do1 adaptors play anti-inflamatory role in pulmonary homeostatis. Genes Cells 2013; 18:56-65
12. Mashima R, Hishida Y, Tezuk, T,Yamanashi Y. Organization of immunoreceptor signaling by adapters. Immunological reviews 2009; 232:273-285.
13. Berger AH, Niki M, Morotti A, Taylor BS, Socci ND, Viale A, Brennan C, Szoke J, Motoi N, Rothman PB, Teruya-Feldstein J, Gerald WL, Ladanyi M, Pandolfi PP. Identification of DOK genes as lung tumor suppressors. Nature genetics 2010;42:216-223.
14. Oxley CL, Anthis NJ, Lowe ED, Vakonakis I, Campbell ID, Wegener KL. An

ACCEPTED MANUSCRIPT

integrin phosphorylation switch: the effect of beta3 integrin tail phosphorylation on Dok1 and talin binding. J. Biol. Chem. 2008;283:5420-5426.
15. Gupta S, Chit JC, Feng C, Bhunia A, Tan SM, Bhattacharjya S. An alternative phosphorylation switch in integrin β2 (CD18) tail for Dok1 binding. Sci. Rep. 2015;5:11630 doi: 10.1038/srep11630
16. Fu H, Subramanian RR, Masters SC. 14-3-3 proteins: structure, function, and regulation. Annu. Rev. Pharmacol. Toxicol. 2000;40:617-647.
17. Fagerholm S, Morrice N, Gahmberg CG, Cohen P. Phosphorylation of the cytoplasmic domain of the integrin CD18 chain by protein kinase C isoforms in leukocytes. J. Biol. Chem. 2002;277:1728-1738.
18. Takala H, Nurminen E, Nurmi SM, Aatonen M, Strandin T, Takatalo M, Kiema T, Gahmberg CG, Ylanne J, Fagerholm SC. Beta2 integrin phosphorylation on Thr758 acts as a molecular switch to regulate 14-3-3 and filamin binding. Blood 2008;112:1853-1862.
19. Chatterjee, D., Zhiping, L. L., Tan, S. M., and Bhattacharjya, S. Interaction analyses of the integrin β2 cytoplasmic tail with the F3 FERM domain of talin and 14-3-3ζ reveal a ternary complex with phosphorylated tail. (2016) J. Mol. Biol. 2016;428: 4129-4142.
20. Shi N, Ye S, Bartlam M, Yang M, Wu J, Liu Y, Sun F, Han X, Peng X, Qiang B, Yuan J, Rao Z. Structural basis for the specific recognition of RET by the Dok1 phosphotyrosine binding domain J. Biol. Chem. 2004;279:4962-4969.
21. Palmer AG 3rd. NMR characterization of the dynamics of biomacromolecules. Chem Rev. 2004;104:3623-3640.
22. Law DA, Nannizzi-Alaimo L, Phillips DR. Outside-in integrin signal transduction alpha IIb beta 3-(GP IIb IIIa) tyrosine phosphorylation induced by platelet aggregation. J. Biol. Chem. 1996;271:10811-10815.
23. Anthis NJ, Haling JR, Oxley CL, Memo M, Wegener KL, Lim CJ, Ginsberg MH, Campbell ID. J. Biol. Chem. 2009;284:36700-36710.
24. Parise LV, Criss AB, Nannizzi L, Wardell MR. Glycoprotein IIIa is phosphorylated in intact human platelets. Blood 1990;75:2363-2368.
25. Lerea KM, Cordero KP, Sakariassen KS, Kirk RI, Fried VA. Phosphorylation sites in the integrin beta3 cytoplasmic domain in intact platelets. J Biol Chem. 1999;274:1914-1919.
26. Sluchanko NN. Association of multiple phosphorylated proteins with the 14-3-3 regulatory hubs: problems and perspectives J Mol Biol. 2018;430:20-26.
27. Hartman AM, Hirsch AKH Molecular insight into specific 14-3-3 modulators: inhibitors and stabilisers of protein-protein interactions of 14-3-3. Eur J Med Chem. 2017;136:573-584.
28. Chen M, Liu T, Xu L, Gao X, Liu X, Wang C, He Q, Zhang G, Liu L. Direct interaction of 14-3-3ζ with ezrin promotes cell migration by regulating the formation of membrane ruffle. J. Mol. Biol. 2014;426:3118-3133.
29. Andrews RK, Harris SJ, McNally T, Berndt MC. Binding of purified 14-3-3 zeta signaling protein to discrete amino acid sequences within the cytoplasmic domain of the platelet membrane glycoprotein Ib-IX-V complex. Biochemistry 1998; 37:638-647.
30. Petosa C, Masters SC, Bankston LA, Pohl J, Wang B, Fu H, Liddington RC. 14-3-3zeta binds a phosphorylated Raf peptide and an unphosphorylated peptide via its conserved amphipathic groove. J. Biol. Chem. 1998;273:16305-16310.
31. Henriksson ML, Francis MS, Peden A, Aili M, Stefansson K, Palmer R, Aitken A, Hallberg B. A nonphosphorylated 14-3-3 binding motif on exoenzyme S that is

ACCEPTED MANUSCRIPT

functional in vivo. Eur J Biochem. 2002;269:4921-4929.
32. Seimiya H, Sawada H, Muramatsu Y, Shimizu M, Ohko K, Yamane K, Tsuruo T. Involvement of 14-3-3 proteins in nuclear localization of telomerase. EMBO J. 2000;19:2652-2661.
33. Bonet R, Vakonakis I, Campbell ID. Characterization of 14-3-3-ζ Interactions with integrin tails. J. Mol. Biol. 2013;425:3060-3072.
34. Obsil T, Ghirlando R, Klein DC, Ganguly S, Dyda F. Crystal structure of the 14-3-3zeta:serotonin N-acetyltransferase complex. a role for scaffolding in enzyme regulation.Cell. 2001;105:257-267.
35. Nakamura F, Stossel TP, Hartwig JH. The filamins, organizers of cell structure and
function. Cell Adh Migr, 2001;5:160-169.
36. Liu J, Das M, Yang J, Ithychanda SS, Yakubenko VP, Plow EF, Qin J. Structural mechanism of integrin inactivation by filamin. Nat Struct Mol Biol. 2015;22:383-389.
37. Bledzka K, Liu J, Xu Z, Perera HD, Yadav SP, Bialkowska K, Qin J, Ma YQ, Plow EF. Spatial coordination of kindlin-2 with talin head domain in interaction with integrin β cytoplasmic tails. J Biol Chem. 2012;287:24585-24594.

Figure 1. Mapping interactions of Dok1 and 14-3-3ζ. (a) Overlay of ^{15}N-^{1}H HSQC spectra of ^{15}N labelled Dok1 PTB domain alone (blue contour) and with sequential additions of 14-3-3ζ at 1:1 (red contour) and 1:2 (green contour) in buffer containing 20 mM sodium phosphate and 50 mM NaCl (pH 6.4). (b) Bar diagram showing normalized residual intensity of each residue of Dok1 PTB domain in presence of 14-3-3ζ at 1:0.5. The line (in red) marked average value of residual intensity. (c) A ribbon representation of the 3-D structure of PTB domain of Dok1 (in two orientations). Residues that showed residual intensity $\leq$0.2 upon addition of 14-3-3ζ are marked in red.

Figure 2. Dok1/14-3-3ζ interactions and R_2 dynamical changes of Dok1 PTB. (a) Bar diagram showing transverse relaxation rate (R_2) of residues of Dok1 PTB domain. (b) Bar diagram showing transverse relaxation rate (R_2) of residues of Dok1 PTB domain in interactions with 14-3-3ζ (1:0.1 molar ratio). (c) Bar diagram showing difference in R_2 values (Dok1/14-3-3ζ and Dok1) of residues of Dok1 PTB domain.

Figure 3. Thermodynamics of interactions of 14-3-3ζ and Dok1 PTB. ITC titrations of binding of Dok1 PTB with 14-3-3ζ. In these experiments, 14-3-3ζ (cell) were titrated with

ACCEPTED MANUSCRIPT

fixed concentration of Dok1 PTB (see Table 1) in buffer containing 20 mM sodium phosphate and 50 mM NaCl (pH 6.4).

Figure 4. Interaction analyses of Dok1 PTB, 14-3-3ζ and pYβ3 CT. (a) Overlay of ^{15}N-^{1}H HSQC spectra of Dok1 PTB domain alone (blue contour), in presence of pYβ3 CT at 1:3 ratio (red contour) and with 14-3-3ζ at 1:3:1 ratio (green contour) in buffer containing 20 mM sodium phosphate and 50 mM NaCl (pH 6.4). (b) One-dimensional ^{31}P NMR spectra of pYβ3 CT in complex of Dok1 PTB domain, 14-3-3ζ and 14-3-3ζ+Dok1 PTB. In these experiments, pYβ3 CT, concentration 0.25 mM, was titrated with Dok1 (red) and 14-3-3ζ (black) at 1:0.5 ratio and in an equimolar Dok1:14-3-3ζ at 1:0.5:0.5 in a buffer solution containing 20 mM tris-HCl and 50 mM NaCl (pH 6.4). ITC thermograms of pYβ3 CT binding with Dok1 PTB (panel c) and Dok1+14-3-3ζ (panel d). ITC parameters are provided in Table 1.

Figure 5. Interactions of Dok1 PTB, 14-3-3ζ and pTβ3 CT. (a) Overlay of ^{15}N-^{1}H HSQC spectra of Dok1 PTB domain alone (blue contour), in presence of pTβ3 CT at 1:3 ratio (red contour) and with 14-3-3ζ at 1:3:1 ratio (green contour) in buffer containing 20 mM sodium phosphate and 50 mM NaCl (pH 6.4). (b) One dimensional ^{31}P spectra of pTβ3 CT, concentration 0.25 mM, with Dok1 PTB domain 1:0.5 (red) and sequential addition of 14-3-3ζ at 1:0.5:0.2 (black) and 1:0.5:0.2 (magenta) in buffer containing 20 mM Tris-HCl and 50 mM NaCl (pH 6.4).

Figure 6. Interaction analyses of Dok1 PTB, 14-3-3ζ and pTβ2 CT. (a) Overlay of ^{15}N-^{1}H HSQC spectra of Dok1 PTB domain alone (blue contour), in presence of pTβ2 CT at 1:3 ratio (red contour) and with 14-3-3ζ at 1:3:1 ratio (green contour) in buffer containing 20 mM sodium phosphate and 50 mM NaCl (pH 6.4). (b) One dimensional ^{31}P spectra of pTβ2 CT, concentration 0.25 mM, with 14-3-3ζ at 1:0.5 and with equimolar mixture of, 1:0.5:0.5,

ACCEPTED MANUSCRIPT

of 14-3-3ζ and Dok1 PTB in buffer containing 20 mM Tris-HCl and 50 mM NaCl (pH 6.4). (c) ITC thermogram of pTβ2 CT binding with Dok1+14-3-3ζ. ITC parameters are provided in Table 1.

Figure 7. Interaction analyses of Dok1 PTB, 14-3-3ζ and pSβ2 CT. (a) Overlay of ^{15}N-^{1}H HSQC spectra of Dok1 PTB domain alone (blue contour), in presence of pSβ2 CT at 1:3 ratio (red contour) and with 14-3-3ζ at 1:3:1 ratio (green contour) in buffer containing 20 mM sodium phosphate and 50 mM NaCl (pH 6.4). (b) ^{31}P NMR spectra of pSβ2 CT alone and in complex of Dok1 PTB, at 1:0.5 ratio and Dok1 PTB+14-3-3ζ, at 1:0.5:0.5 ratio in buffer solution containing 20 mM tris-HCl and 50 mM NaCl (pH 6.4). (c and d) ITC thermograms of pSβ2 CT binding with Dok1+14-3-3ζ (panel c) and Dok1 PTB (panel d). ITC parameters are provided in Table 1.

Figure 8. Molecular models of 14-3-3ζ/Dok1 PTB complex and phosphorylated β CTs. (a) A ribbon representation of the topology of the complex between dimeric 14-3-3ζ (in green) and Dok1 PTB domain (in cyan). (panels b and c) Potential non-polar, polar and cation–π interactions between the C-terminal helix of 14-3-3ζ and Dok1 PTB domain. Non-polar packing interactions among residues L216, Y212 of 14-3-3ζ with L180 and W156 of Dok1 PTB domain (panel b), potential cation-π interactions between Y174 of Dok1 and R222 of 14-3-3ζ (panel c). (d) A ribbon representation of the overall topology of the ternary complex between dimeric 14-3-3ζ (in green), Dok1 PTB domain (in cyan) and phosphorylated pTβ2 CT (in orange), binding to 14-3-3ζ, and pYβ3 CT (in pink), binding to Dok1 PTB domain.

Figure 9: Proposed model of recruitment of Dok1/14-3-3ζ complex to β2 integrin. Dok1 and 14-3-3ζ forms a complex. Under resting condition, Dok1 binds to pSer756 in integrin ß2 CT, whereas 14-3-3ζ tethers to Dok1. Upon activation, integrin β2 CT pSer756 is dephosphorylated, leading to the release of Dok1. Concomitantly, phosphorylation of Thr758

ACCEPTED MANUSCRIPT

in integrin β2 CT leads to the binding of 14-3-3ζ. Hypothetically, this switchover could be fast because Dok1 and 14-3-3 forms a complex. Other molecules involved in integrin regulation, including filamin A, kindlin-3, migfilin, and talin are shown.

Table 1: ITC interactions analyses of phosphorylated β2 and β3 CTs with Dok1 PTB, 14-3-3ζ/Dok1 complex

Cell Concentration(μM)	Syringe Concentration(μM)	K_d (μM)	ΔH (Kcal/mol)	ΔS (cal/mol/deg)	ΔG (Kcal/mol)	N
14-3-3ζ (20)	Dok1 (700)	294	-18.2	-44.9	-4.80	2.5
Dok1 (30)	pYβ3 (600)	41.8	-17.6	-39.0	-5.94	2.0
Dok1+14-3-3ζ (30)	pYβ3 (800)	16.5	-21.9	-51.6	-6.48	2.5
14-3-3ζ+Dok1 (50)	pTβ2 (900)	12.6	-15.9	-33.3	-6.64	2.1
Dok1 (50)	pSβ2 (500)	24.1	-30.2	-80.4	-6.28	1.65
Dok+14-3-3ζ (50)	pSβ2 (500)	298	-16.5	-39.29	-4.79	0.93

Table 2: Amino acid sequences of the β2 and β3 CTs used in this study. Phosphorylated residue is bold faced in the sequence.

pTβ2 CT	K^{724}-A-L-I-H-L-S-D-L-R-E-Y-R-R-F-E-K-E-K-L-K-S-Q-W-N-N-D-N-P-L-F-K-S-A-**pT**^{758}-T-T-V-M-N-P-K-F-A-E-S^{769}
pSβ2 CT	K^{724}-A-L-I-H-L-S-D-L-R-E-Y-R-R-F-E-K-E-K-L-K-S-Q-W-N-N-D-N-P-L-F-K-**pS**^{756}-A-T-T-T-V-M-N-P-K-F-A-E-S^{769}
pYβ3 CT	R^{736}-A-K-W-D-T-A-N-N-P-L-**pY**^{747}-K-E-A-T-S-T-F-T-N-I-T-Y-R-G-T^{762}
pTβ3 CT	R^{736}-A-K-W-D-T-A-N-N-P-L-Y-K-E-A-**pT**^{751}-S-T-F-T-N-I-T-Y-R-G-T^{762}

ACCEPTED MANUSCRIPT

Highlights

- Beta cytosolic tails (β-CTs) of integrins bind to repressors and activators.
- How repressors and activators could aptly switch positions are not clearly understood.
- Activator 14-3-3ζ and repressor Dok1 forms a binary complex.
- 14-3-3ζ/Dok1 complex acts as a switch toward recognition of phosphorylated β-CTs.
- A novel mode of integrin regulation is presented.

ACCEPTED MANUSCRIPT

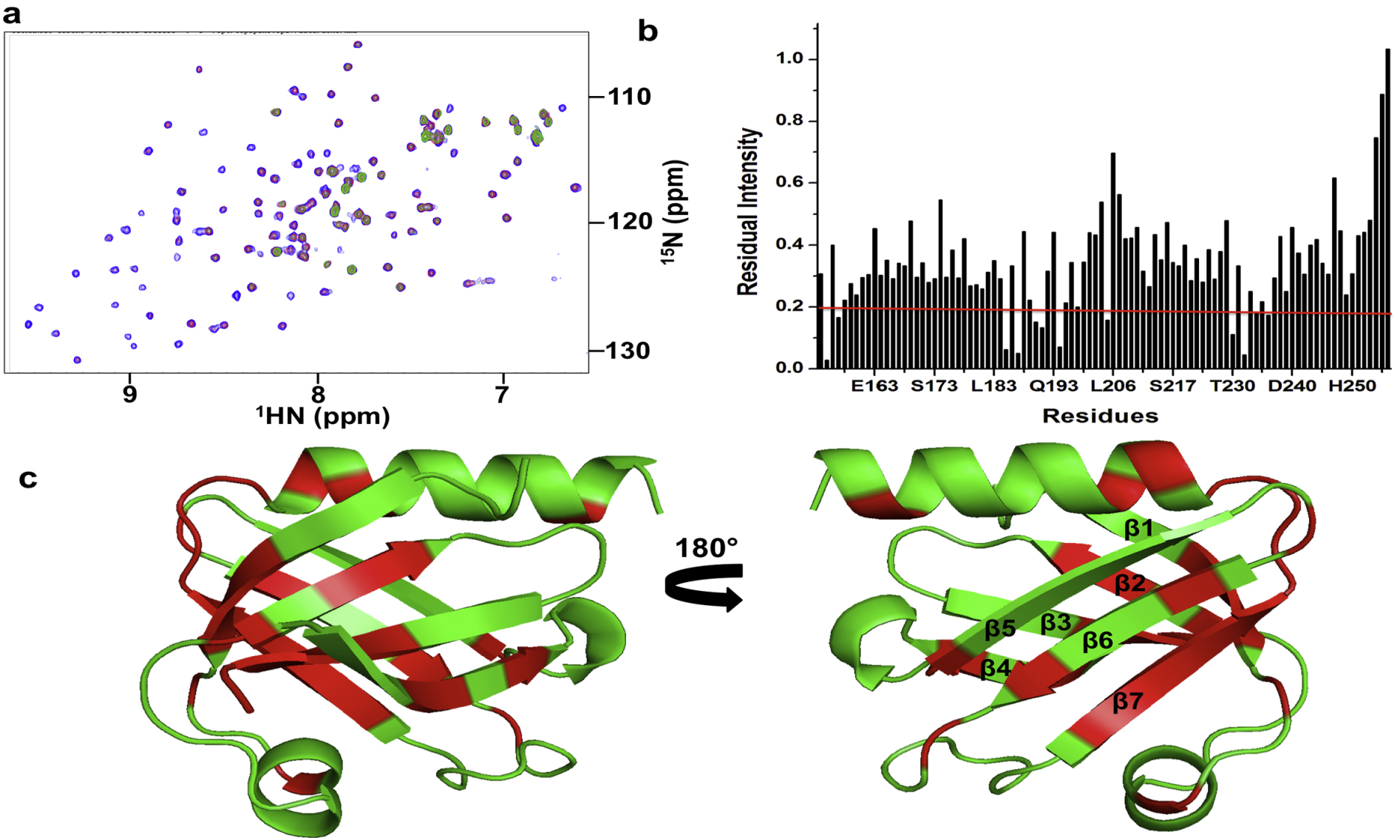

a
110
120
130
^{15}N (ppm)
9
8
7
^{1}HN (ppm)
b
Residual Intensity
1.0
0.8
0.6
0.4
0.2
0.0
E163 S173 L183 Q193 L206 S217 T230 D240 H250
Residues
c
180°
β1
β2
β3
β4
β5
β6
β7

Figure 1

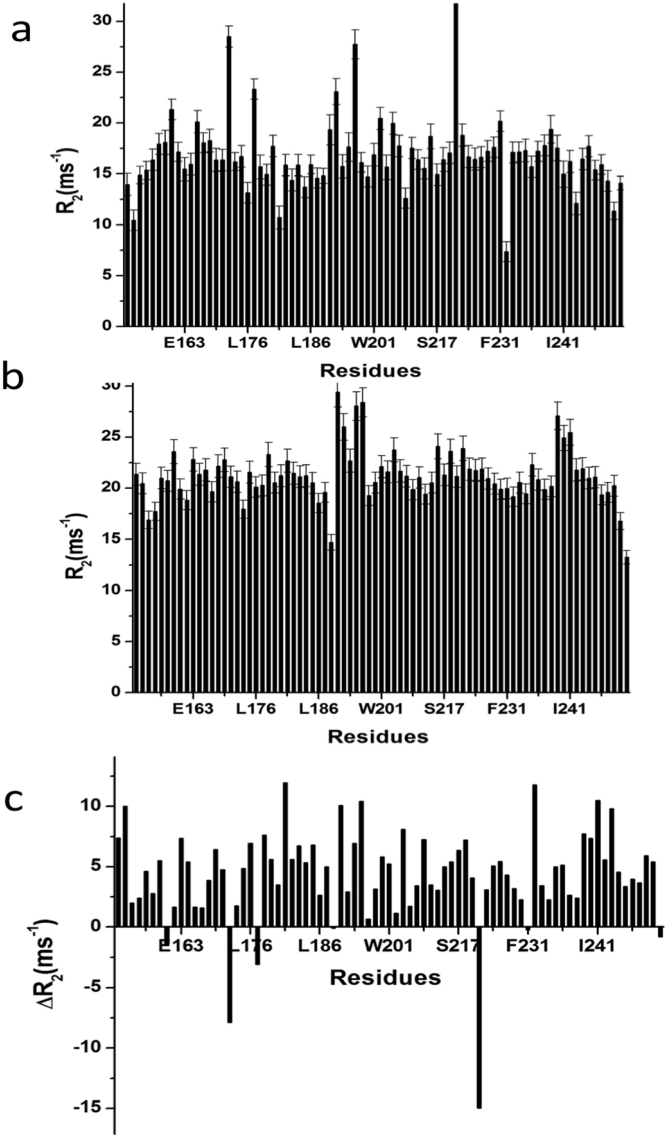

a
$R_2(ms^{-1})$
0
5
10
15
20
25
30
E163
L176
L186
W201
S217
F231
I241
Residues
b
$R_2(ms^{-1})$
0
5
10
15
20
25
E163
L176
L186
W201
S217
F231
I241
Residues
c
$\Delta R_2(ms^{-1})$
-15
-10
-5
0
5
10
E163
L176
L186
W201
S217
F231
I241
Residues

Figure 2

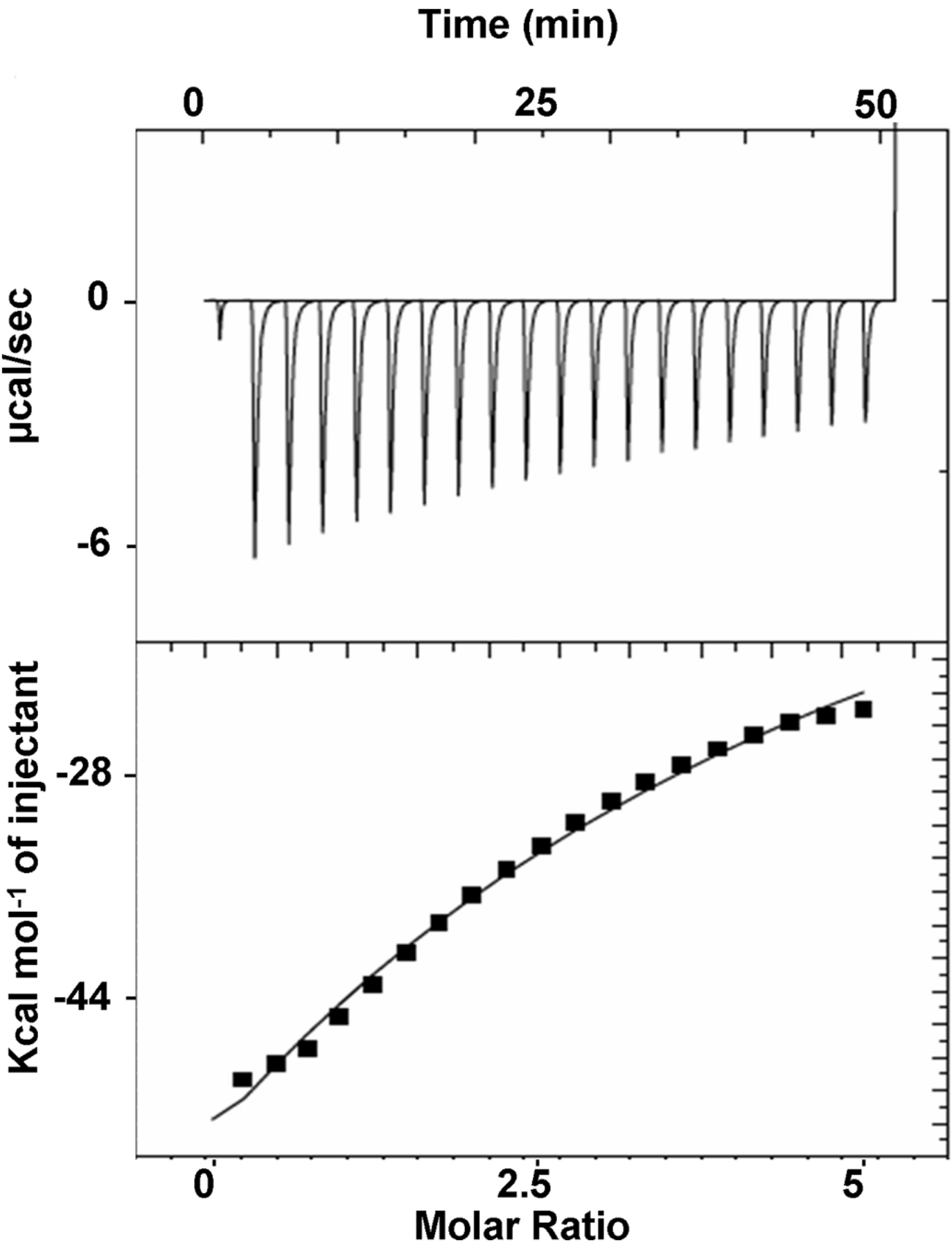

Time (min)
0
25
50
µcal/sec
0
-6
Kcal mol-1 of injectant
-28
-44
0
2.5
5
Molar Ratio

Figure 3

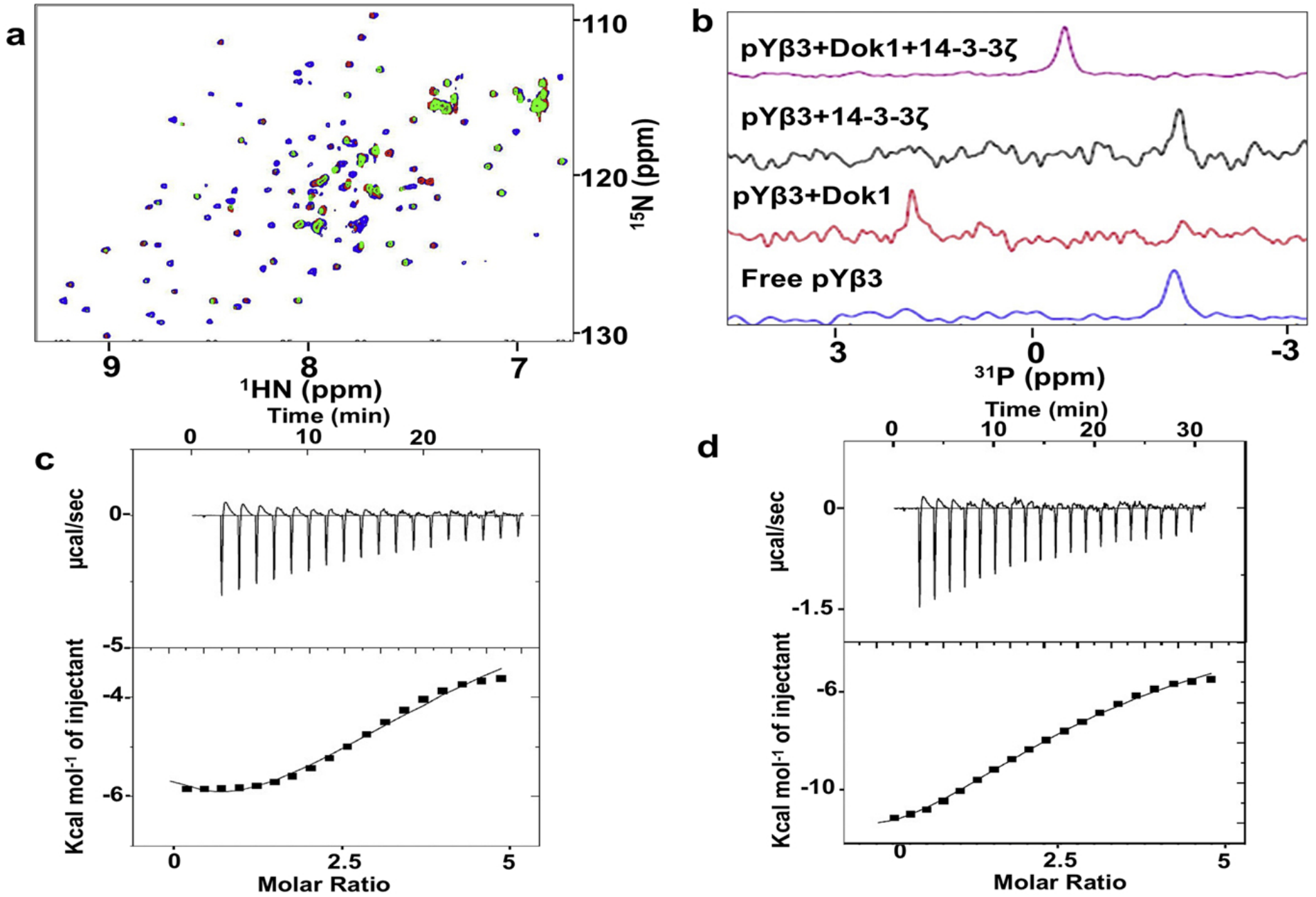

a
110
120
130
^{15}N (ppm)
9
8
7
^{1}HN (ppm)
b
pYβ3+Dok1+14-3-3ζ
pYβ3+14-3-3ζ
pYβ3+Dok1
Free pYβ3
3
0
-3
^{31}P (ppm)
c
Time (min)
0
10
20
µcal/sec
0
-5
Kcal mol^{-1} of injectant
-4
-6
0
2.5
5
Molar Ratio
d
Time (min)
0
10
20
30
µcal/sec
0
-1.5
Kcal mol^{-1} of injectant
-6
-10
0
2.5
5
Molar Ratio

Figure 4

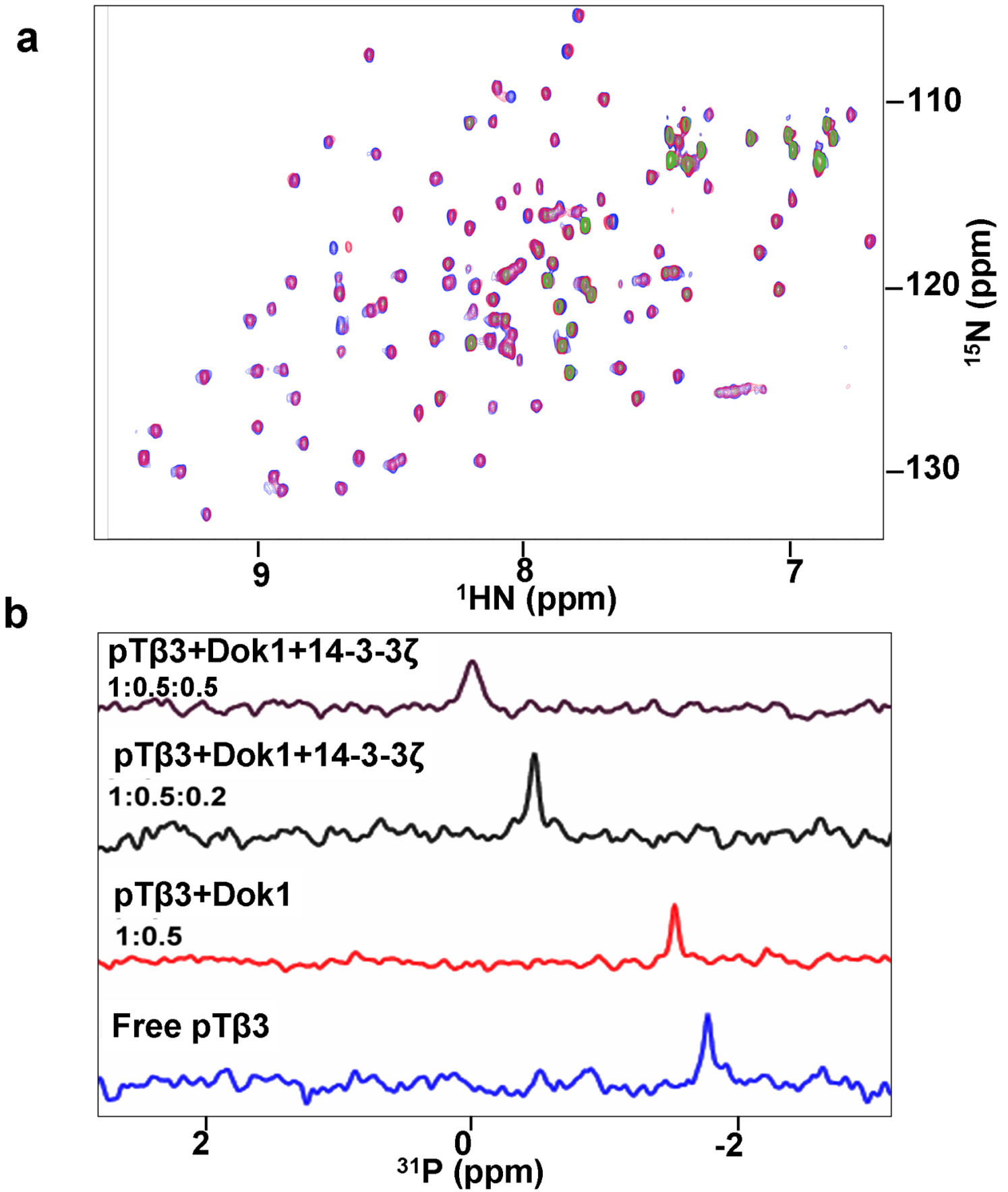

a
110
120
130
15N (ppm)
9
8
7
1HN (ppm)
b
pTβ3+Dok1+14-3-3ζ
1:0.5:0.5
pTβ3+Dok1+14-3-3ζ
1:0.5:0.2
pTβ3+Dok1
1:0.5
Free pTβ3
2
0
-2
31P (ppm)

Figure 5

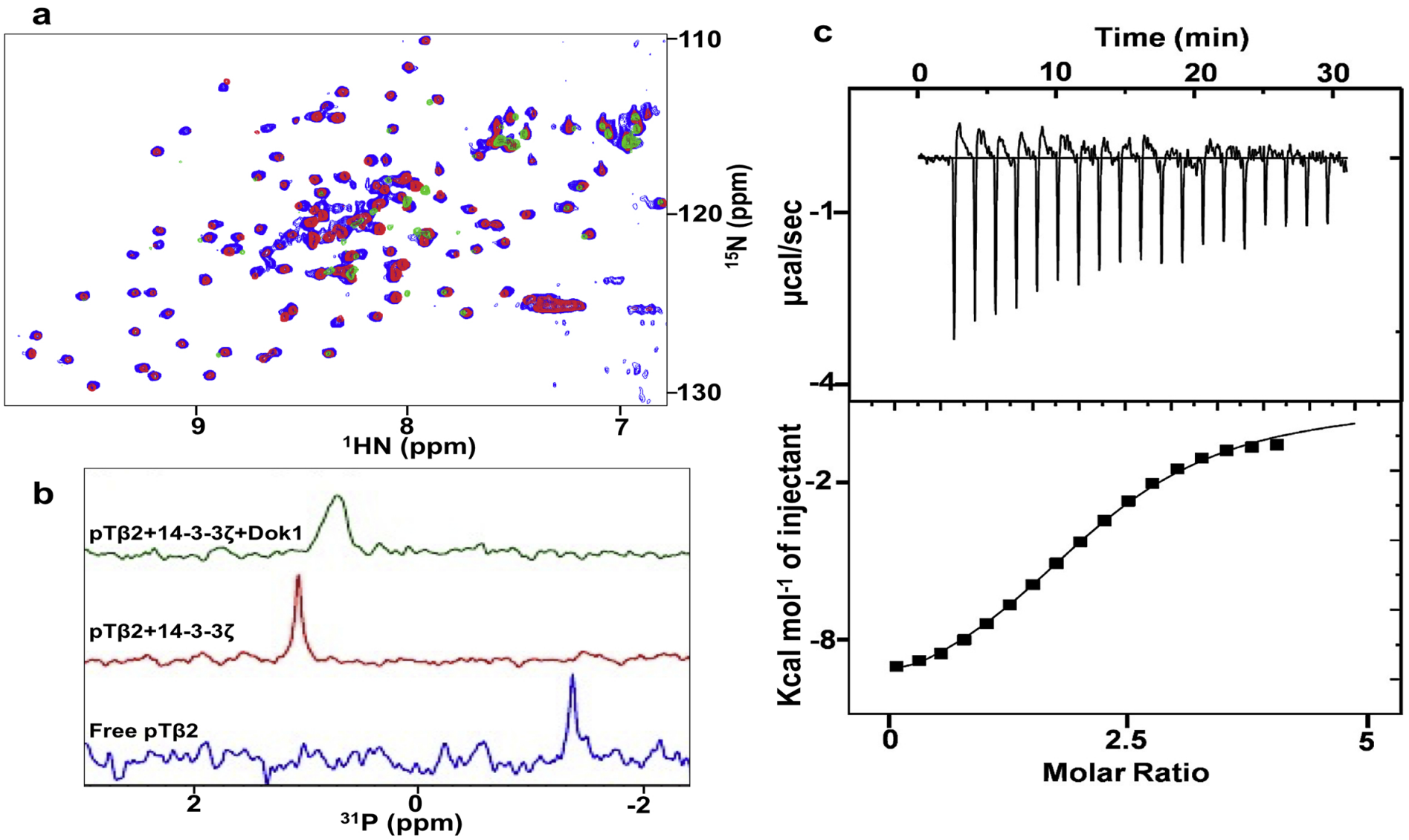

a
110
120
130
15N (ppm)
9
8
7
1HN (ppm)
b
pTβ2+14-3-3ζ+Dok1
pTβ2+14-3-3ζ
Free pTβ2
2
0
-2
31P (ppm)
c
Time (min)
0
10
20
30
µcal/sec
-1
-4
Kcal mol-1 of injectant
-2
-8
0
2.5
5
Molar Ratio

Figure 6

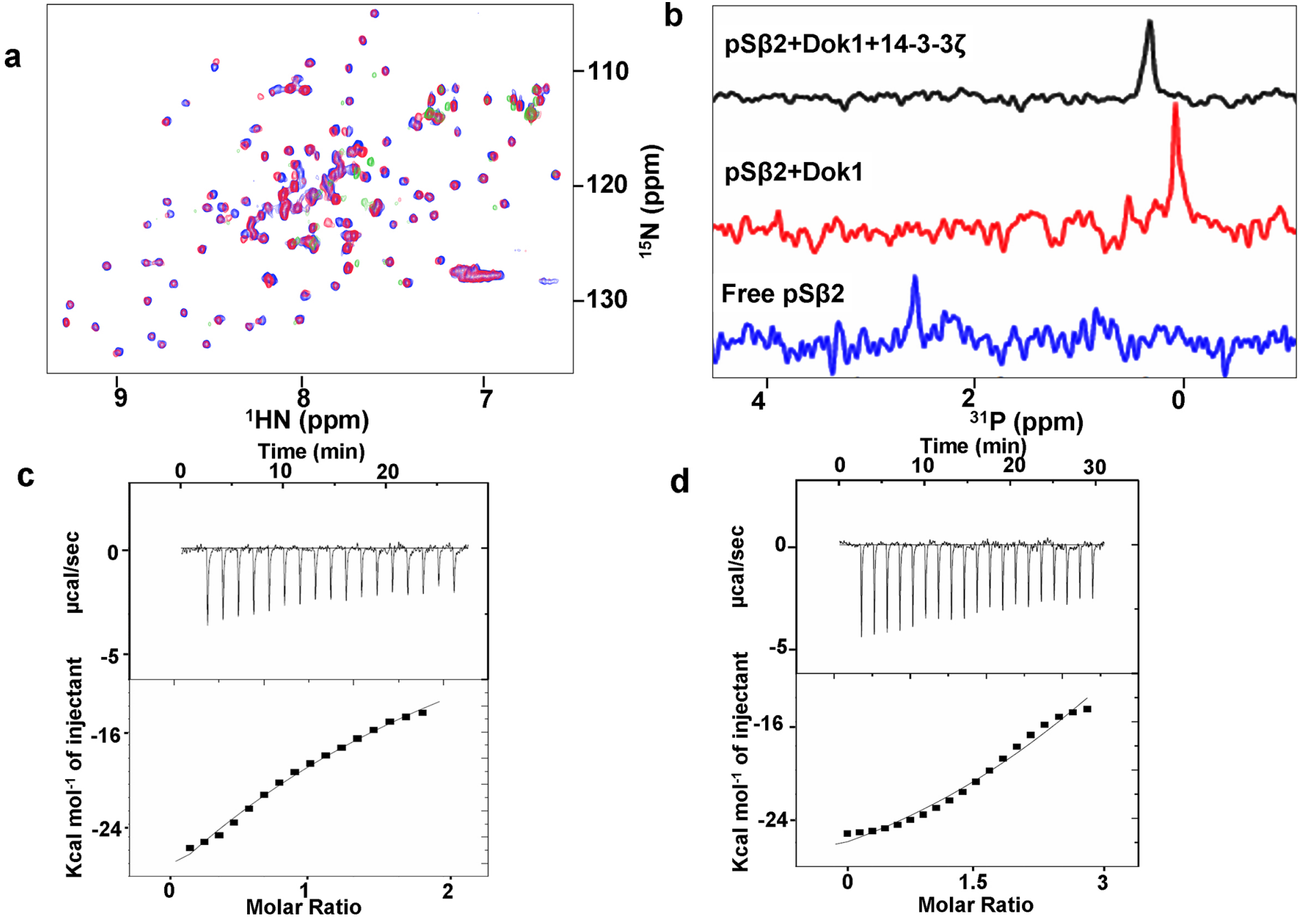

a
110
120
130
^{15}N (ppm)
9
8
7
^{1}HN (ppm)
b
pSβ2+Dok1+14-3-3ζ
pSβ2+Dok1
Free pSβ2
4
2
0
^{31}P (ppm)
c
Time (min)
0
10
20
µcal/sec
0
-5
Kcal mol^{-1} of injectant
-16
-24
0
1
2
Molar Ratio
d
Time (min)
0
10
20
30
µcal/sec
0
-5
Kcal mol^{-1} of injectant
-16
-24
0
1.5
3
Molar Ratio

Figure 7

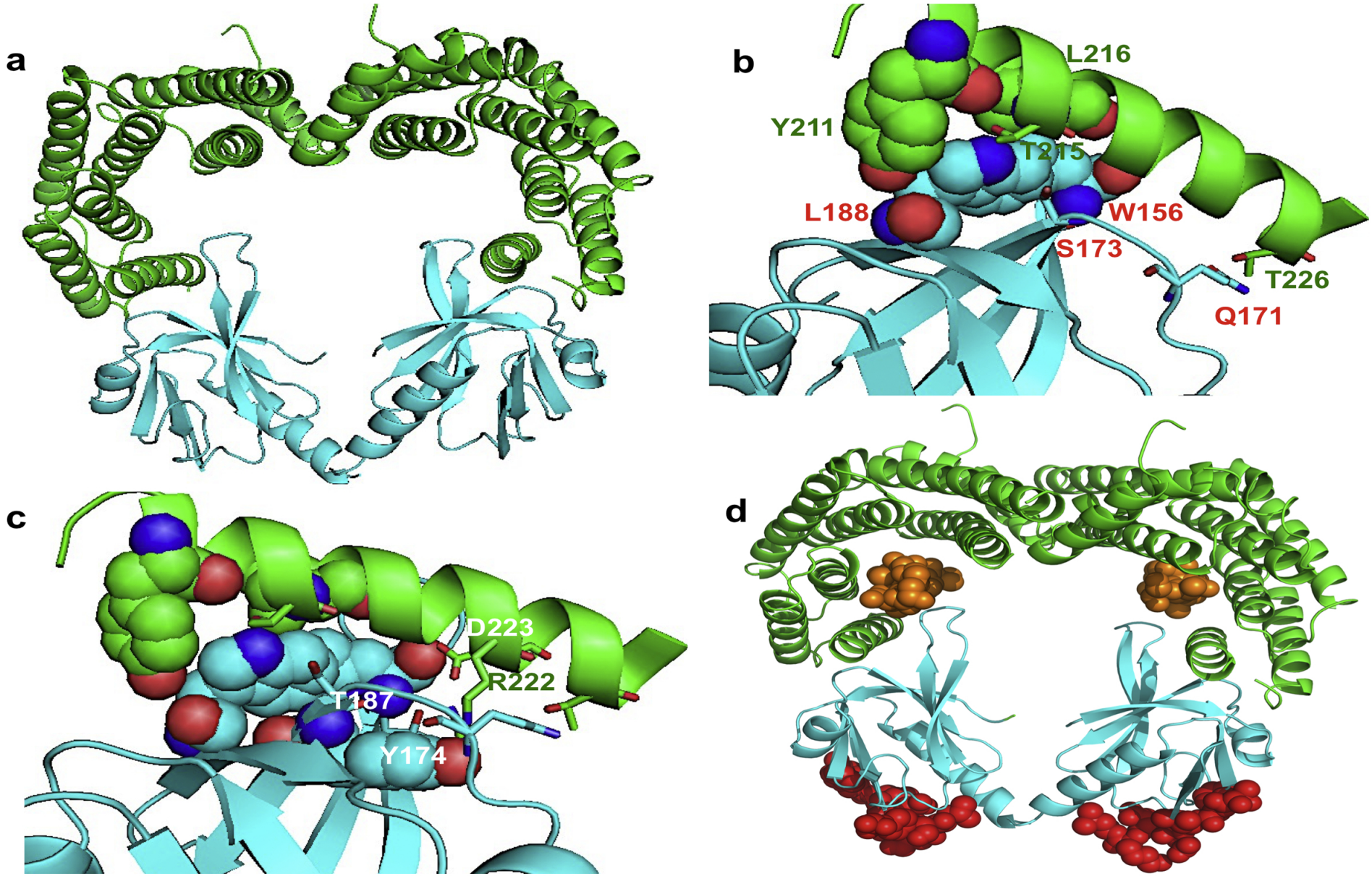

a
b
L216
Y211
T215
L188
W156
S173
T226
Q171
c
D223
R222
T187
Y174
d

Figure 8

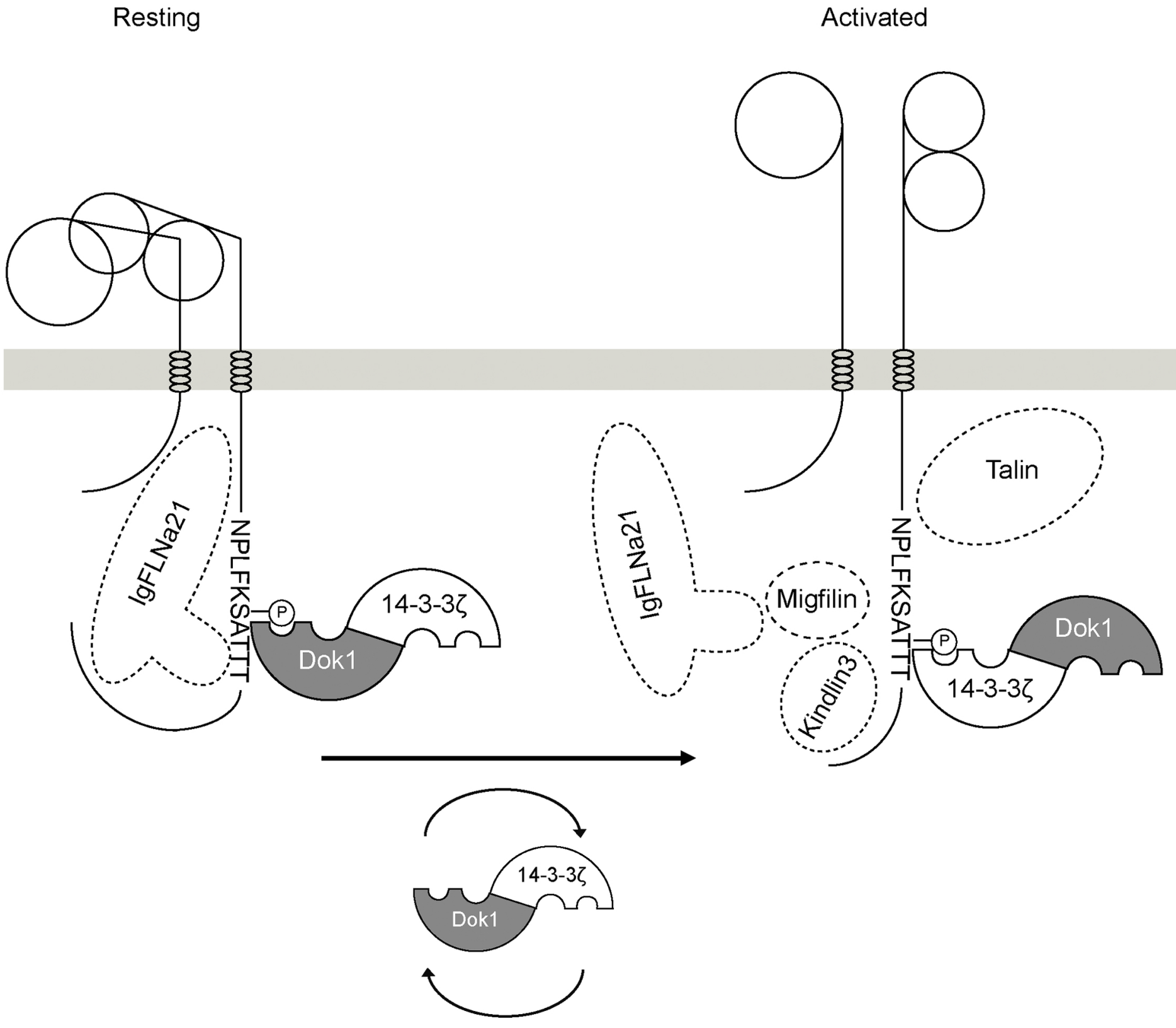

Resting
Activated
IgFLNa21
NPLFKSATTT
P
14-3-3ζ
Dok1
IgFLNa21
Migfilin
Kindlin3
Talin
NPLFKSATTT
P
Dok1
14-3-3ζ
14-3-3ζ
Dok1

Figure 9